From competing motor plans to a single action within a single trial on the human motor periphery

Chao Gu (顾超)[1,2,6], Brian D. Corneil[1-4], W. Pieter Medendorp[5], and Luc P.J. Selen[5]

Departments of [1]Psychology and [3]Phyiology & Pharmacology; University of Western Ontario; London, ON, N6A 5B7; Canada
The [2]Brain and Mind Institute and [4]Robarts Research Institute;
[5]Radboud University, Donders Institute for Brain, Cognition and Behaviour; 6500 HB Nijmegen, The Netherlands
[6]Present Address: Center for Perceptual Systems, The University of Texas at Austin; Austin, TX, 78712, USA

Corresponding Author:
Dr. Luc Selen
l.selen@donders.ru.nl

Key words: motor planning; decision-making; visually-guided reaching; electromyography

Number of Pages: 30
Number of Figures: 6
Words in Abstract: 239
Words in Introduction: 612
Words in Discussion: 1166

Acknowledgement

This work was supported by operating grants from the Natural Sciences and Engineering Research Council of Canada (NSERC) to BDC [RGPIN-311680], the Canadian Institutes of Health Research (CIHR) to BDC [MOP-93796], a Vici grant from the Netherlands Organization for Scientific Research to WPM [453-11-001], a NSERC Alexander Graham Bell Canada Graduate Doctoral Scholarship to CG, and a travel supplement from the Canada Graduate Scholarships – Michael Smith Foreign Study Supplements Program to CG.

ABSTRACT

Contemporary theories of motor control have suggested that multiple motor commands compete for action selection. While most of these competitions are completed prior to movement onset, averaged saccadic eye movements that land at an intermediate location between two visual targets are thought to arise when a movement is initiated prior to the resolution of the competition. In contrast, while averaged reach movements have been reported, there is still debate on whether averaged reach movements are the result of a resolved competition between two potential actions or a strategic behavior that optimally incorporates the current task demands. Here, we use a reach version of the paradigm that has previously shown to elicit saccadic averaging to examine whether similar averaging occurs based on neuromuscular activity of an upper limb muscle. On a single trial basis, we observed a temporal evolution of the two competing motor commands during a free-choice reach task to one of two visual targets. The initial wave of directionally-tuned muscle activity (~100 ms after target onset) was an averaged of the two motor commands which then transformed into a single goal-directed motor command at the onset of the voluntary reach (~200-300 ms after target onset). The transition from an early motor command to a single goal-direct command resembled the fact that saccadic averaging was most prominent for short-latency saccades. Further, the idiosyncratic choice made on a given trial was correlated with the biases in the averaged motor command.

57 **INTRODUCTION**

58 Our environment offers multiple potential motor actions, but ultimately only one action can be
59 selected. So how does our brain decide between these potential motor actions? Classical theories
60 of decision-making assume a two-stage process, in which the brain first selects an appropriate
61 action and then plans the desired motor commands to execute the selection action (Donders,
62 1969; McClelland, 1979). However, neurophysiological studies have shown that multiple
63 potential motor plans can be concurrently encoded within brain regions involved in eye (Bichot
64 et al., 1996, 2001; Basso and Wurtz, 1997; McPeek and Keller, 2002) or reach movements
65 (Cisek and Kalaska, 2005; Cui and Andersen, 2011; Klaes et al., 2011). Further, these potential
66 motor plans are thought to compete for selection at the neurophysiological level (Schall, 2001;
67 Cisek, 2007). There are behavioral indicators that are thought to arise from such competitions.
68 For example, when participants are free to look to either one of two suddenly appearing visual
69 targets (i.e. a free-choice task), they often generate an initial saccade that lands somewhere in
70 between the two targets (Findlay, 1982; He and Kowler, 1989; Chou et al., 1999). The extent of
71 this *saccadic averaging* is inversely correlated with saccadic reaction time (RT), where saccadic
72 averaging is most prominent for short-latency RT trials (Ottes et al., 1984; Walker et al., 1997).
73 The dependency of RT for saccadic averaging is thought to arise because the saccade is initiated
74 prior to the competition between the two different motor plans being resolved.

75 While there is clear evidence for competition and averaging within the oculomotor
76 system, it is less clear whether a similar competition between motor plans influences reaching
77 behavior. Averaged reaching movements can be evoked in a 'go-before-you-know' task, where
78 information about the true target is only provided after reach movement onset (Chapman et al.,
79 2010; Stewart et al., 2014; Gallivan et al., 2017). However, these averaged reach movements can

80 be abolished by changes to either task instructions or constraints (Hudson et al., 2007; Chapman
81 and Goodale, 2010), suggesting that the averaged movement may reflect an optimal task strategy
82 rather than a competition between two motor plans (Wong and Haith, 2017). More
83 fundamentally, the neurophysiological evidence for multiple potential reach plans has recently
84 been questioned (Dekleva et al., 2018) in that the observed averaging may be an artifact caused
85 by combining neural activity across multiple trials rather than examining activity on an
86 individual trial-by-trial basis. Thus, it is still debated whether similar rules apply for saccades
87 and reaches when the brain has to resolve multiple potential motor plans.

88 Our approach here is to use the same paradigm that has previously been shown to elicit
89 saccadic averaging and look for signatures of averaging during visually-guided reaches. In this
90 paradigm, participants are free to reach towards one of two visual targets that appear
91 concurrently (**Fig. 1b, c**, *Free-Choice Task*). Unlike the 'go-before-you-know' task (Chapman et
92 al., 2010), there is nothing to be gained by strategically aiming between the two potential
93 locations (Wong and Haith, 2017) and thus any observed averaging can be attributed to an
94 unresolved competition between two reach plans. By examining electromyographic (EMG)
95 activity from an upper limb muscle during this free-choice task, we observed a transition from an
96 initial averaged motor command (~100 ms after target onset) into a goal-directed reach
97 movement towards a single selected target (~200-300 ms after target onset). Further, the
98 participant's idiosyncratic choices on a given trial correlated with the bias observed in the initial
99 averaged motor command (Pastor-Bernier and Cisek, 2011). Thus, our results suggest that the
100 initial wave of upper limb muscle recruitment is a readout of a still unresolved competition
101 between the two reach movements, similar to that previously observed for averaged saccades.

MATERIALS AND METHODS

Participants and Procedures

The experiment was conducted with approval from the institutional ethics committee from the Social Sciences faculty at Radboud University Nijmegen, The Netherlands. 12 participants (eight females and four males), between 18 and 33 years of age (mean ± SD = 24 ± 5), gave their written consent prior to participating in the experiment. Three participants (one female and two males) were self-declared left-handed, while the remaining participants were self-declared right-handed. All participants were compensated for their time with either course credits or a monetary payment and they were free to withdraw from the experiment at any time. All participants had normal or corrected-to-normal vision and had no known motor impairments.

Reach Apparatus and Kinematic Acquisition

Participants were seated in a chair in front a robotic rig. The participant's right arm was supported by an air-sled floating on top of a glass table. All participants performed right-handed horizontal planar reaching movements while holding the handle of the planar vBOT robotic manipulandum (Howard et al., 2009).). The vBOT measured both the *x*- and *y*-positions of the handle at a 1 kHz sampling rate. Throughout the whole experiment a constant load of 5 N in the rightward direction, relative to the participant, was applied to increase the baseline activity for the right pectoralis muscle (see below). All visual stimuli were presented within the plane of the horizontal reach movements via a semi-silver mirror, which reflected the display of a downward facing LCD monitor (Asus – model VG278H, Taipei, Taiwan). The start position and the peripheral visual targets were presented as white circles (0.5 and 1.0 cm radii, respectively) onto

124 a black background. Real-time visual feedback of the participant's hand position was given
125 throughout the experiment and was represented by a yellow cursor (0.25 cm in radius).
126
127 *EMG Acquisition*
128 EMG activity was recorded from the clavicular head of the right pectoralis major (PEC) muscle
129 using wireless surface EMG electrodes (Trigno sensors, Delsys Inc., Natick, MA, USA). The
130 electrodes were placed ~1 cm inferior to the inflection point of the participant's right clavicle.
131 Concurrent with the EMG recordings, we also recorded a photodiode signal that indicated the
132 precise onset of the peripheral visual targets on the LCD screen. Both the EMG and photodiode
133 signals were digitized and sampled at 1.11 kHz.
134
135 *Experiment Paradigm*
136 Each trial began with the onset of the start position located at the center of the screen, which was
137 also aligned with the participant's midline. Participants had to move their cursor into the start
138 position and after a randomized delay period (1-1.5 sec) either one (*Single Target*, 25% of all
139 trials, **Fig. 1a**) or two peripheral targets appeared (*Double Targets*, 75%). All peripheral targets
140 were presented 10 cm away from the start position and at one of 12 equally spaced locations
141 (dotted circles in **Fig. 1a**). The onset of the peripheral targets occurred concurrently with the
142 offset of the start position. Participants were explicitly instructed to reach as fast as possible
143 towards one of the peripheral target locations during *Double Target* trials. The trial ended as
144 soon as the cursor entered one of the peripheral targets. To ensure that the participants reached as
145 fast as possible, the peripheral targeted turned red if the cursor had not moved out of the start

146 position within 500 ms after the onset of the peripheral target. Participants were not given any
147 instructions of where to look and eye movements were not tracked during the experiment.
148 Each experiment consisted of eight blocks, with each block containing 240 trials, with 60
149 *Single Target* and 180 *Double Target* trials, pseudo-randomly interleaved. For the *Double Target*
150 trials, the two targets appeared either 60°, 120°, or 180° apart in equal likelihood. Every possible
151 single and double target configuration was presented five times in every block, resulting in 40
152 repetitions over the whole experiment.
153
154 *Data Analyses*
155 All data were analyzed using custom-written scripts in Matlab (version R2014b, Mathworks Inc.,
156 Natick, MA, USA). For both the 60° and 120° *Double Target* trials, we sorted trials based on
157 whether the final reach was directed to either the CW (**Fig. 1b**, red arrow) or CCW target (blue
158 arrow). Thus, for all CW and CCW reach trials the non-chosen target direction was in the CCW
159 and CW directions, respectively. Trials from the 180° *Double Target* condition cannot be sorted
160 in this way, since the non-chosen target direction was always 180° away.
161
162 *Reach onset detection and initial reach direction:* Reach onset was identified as the first time-
163 point after the onset of the peripheral targets at which the tangential hand velocity exceeded two
164 cm/sec. Reach RT was calculated as the time between the onset of the peripheral targets and the
165 initiation of the reach movement. Initial reach direction was quantified as the angular direction of
166 the vector connecting the start position and the location of the hand at the time of reach onset.
167 From this, initial reach error was defined as the angular difference between the initial reach
168 direction and the direction of the chosen target.

EMG processing: All EMG data were first rectified and aligned to both the onset of the peripheral targets (as measured by the onset of the photodiode) and reach initiation. To account for the differences in EMG recordings across the participants, we first normalized EMG activity for each participant by dividing against their own mean baseline activity (i.e. mean EMG activity over the 40 ms window prior to the stimuli onset). We then log-normalized each participant's EMG activity to account for the non-linearity of EMG activity. We specifically examined two distinct waves of EMG activity: (1) The initial *stimulus-locked response* (*SLR*) that occurs 85-125 ms evoked by the onset of the visual stimuli (Gu et al., 2016, 2018, 2019), and (2) the later movement-related response (MOV, -20 to 20 ms around reach initiation) associated with the onset of the reach movement. To prevent any overlap between these two different epochs, we excluded all trials with RTs less than 185 ms (~7% of all trials). We also excluded trials with RTs greater than 500 ms (<0.1% of all trials).

Receiver-Operating Characteristic Analysis: As done previously (Corneil et al., 2004; Pruszynski et al., 2010), we used a time-series receiver-operating characteristic (ROC) analysis to quantitatively detect the presence of a SLR. To do this, we first separated leftward (target directions between 120° to 240°) and rightward (–60° to 60°) *Single Target* trials. For each time-point from 100 ms before to 300 ms after stimulus onset, we calculated the area under the ROC curve between the EMG activity for leftward compared to rightward trials. This metric indicates the probability that an ideal observer could discriminate the stimulus direction based solely on the distribution of EMG activity at that given time-point. A value of 0.5 indicates chance discrimination, whereas a value of 1 or 0 indicates perfectly correct or incorrect discrimination,

192 respectively. We set the threshold for discrimination at 0.6, as this criterion exceeds the 95%
193 confidence intervals for EMG data that has been randomly shuffled through a bootstrapping
194 procedure (Chapman and Corneil, 2011). The discrimination time was defined as the time after
195 stimulus onset at which the ROC was above 0.6 and remained above that threshold for at least
196 five out of the next 10 samples. We defined any participant with a discrimination time less than
197 125 ms as a participant exhibiting a SLR. Based on this criterion, 11 of the 12 participants had a
198 detectable SLR. All subsequent analyses were done on the 11 participants with a SLR.
199
200 *Directional Tuning of EMG activity:* We assumed cosine tuning (**Eq. 1**) between the log-
201 normalized EMG activity and the chosen target direction for both the SLR and MOV epochs:
202 $$EMG(x) = A \times cos(x - \theta)$$ **Equation 1**
203 in which x is the chosen target direction in degrees, starting CCW from straight right; $EMG(x)$ is
204 the log-normalized EMG activity for the given target direction; A is the amplitude of the cosine
205 tuning; and θ is the preferred direction (PD) of the EMG activity. We used Matlab's curve fitting
206 toolbox *fit* function to estimate both the A and θ parameters. We constrained our search
207 parameters such that $A > 0$ and $0° \leq \theta < 360°$. The initial values of the parameters were $A = 1$
208 and $\theta = 180°$. PDs of 0° and 180° would represent straight rightward and leftward, respectively.
209
210 *Model predictions:* Previous studies have proposed different models of how the brain converts
211 multiple visual stimuli into a motor command. Here to drive the predictions for the *Double*
212 *Target* models, we used the *Single Target* data and assumed a non-linear cosine tuning between
213 target direction and reach direction (**Fig. 2a**). Each model used parameters derived from each

214 participant's own *Single Target* data to predict both the PD and amplitude of the cosine tuning
215 curves for *Double Target* trials. Thus, no free parameters were fitted in any of these four models.
216 **Model 1:** The *winner-take-all model* (**Fig. 4a**) assumes that only the target direction that
217 the participant reaches towards is converted into a motor command. Therefore,
218 $EMG(x_1|x_1, x_2) = EMG(x_1)$, where x_1 and $x_2$are the chosen and non-chosen target directions,
219 respectively.
220 **Model 2:** The *spatial averaging model* (**Fig. 4b**) assumes that the two potential target
221 directions are first spatially averaged into an intermediate target direction. Then that target
222 direction is converted into a motor command. Therefore, $EMG(x_1|x_1, x_2) = EMG\left(\frac{x_1+x_2}{2}\right)$.
223 **Model 3:** The *motor averaging model* (**Fig. 4c**) assumes that the two potential target
224 directions are first converted into their own distinct motor commands and then averaged into a
225 single motor command. Therefore, $EMG(x_1|x_1, x_2) = 0.5 \times EMG(x_1) + 0.5 \times EMG(x_2)$.
226 **Model 4:** The *weighted motor averaging model* (**Fig. 4d**) is a variation of the motor
227 averaging model. It assumes that the two target directions are converted into their associated
228 motor commands, but that they are differentially weighted into the final averaged motor
229 command. A higher weight is assigned to the chosen target compared to the non-chosen target
230 direction. To estimate these weights, we used each participant's own *Single Target* data.
231 Previous works have shown that the SLR magnitude is negatively correlated with the ensuing RT
232 for single target visually-guided reaches (Pruszynski et al., 2010; Gu et al., 2016). We assumed
233 that the trial-by-trial magnitude of the SLR reflected the 'readiness' to move towards the target
234 direction. Thus, we took the median RT split of the *Single Target* data to get cosine tuning for
235 both *Fast* and *Slow RT* trials. This results in *Fast RT* and *Slow RT* amplitude and PD estimates.
236 We then used these parameters to compute the tuning curves for the *Double Target* trials. The

Fast RT tuning curve parameters were used for the chosen target direction and the *Slow RT* tuning curve parameters were used for the non-chosen target direction. Therefore, $EMG(x_1|x_1, x_2) = 0.5 \times EMG_{Fast}(x_1) + 0.5 \times EMG_{Slow}(x_2)$.

To quantify the goodness-of-fit for each model, we calculated the mean squared error (MSE) between the predicted and observed PD and normalized amplitude for each participant. Due to the non-linear interaction between PD and normalized amplitude, we evaluated the total fit error. To do this, we took the sum of the MSE between the predicted and observed cosine tuning for each of the 12 different target reach directions (i.e. x_1 = 0°, 30°, 60°, … 330°).

Statistical Analyses

Statistical analyses were performed using either one or two-sample *t*-tests or a one-way ANOVA. For all post-hoc comparisons, we used a Tukey's HSD correction. The statistical significance was set as $P < 0.05$. For the model comparison, significance was set at $P < 0.0083$, Bonferroni corrected for the six possible comparisons between the four different models.

RESULTS

Participants sat at a desk and used their right hand to interact with the handle of a robotic manipulandum (Howard et al., 2009) that controlled the position of a virtual cursor presented on a horizontal mirror reflecting a downward facing LCD screen. Participants performed a free-choice goal-directed right-handed reach movements in response to the onset of either one (**Fig. 1a**, *Single Target*) or two visual stimuli (**Fig. 1b** and **c**, *Double Target* trials) that appeared simultaneously. The visual target pseudo-randomly appeared at 12 different possible directions equally spaced around the start position. During *Double Target* trials, the two visual stimuli had

260 an angular separation of either 60°, 120°, or 180°. All conditions and target configurations were
261 randomly interleaved. Throughout the experiment, we measured EMG activity from the PEC
262 muscle.

263 Prior to examining the *Double Target* trials, we will first describe PEC EMG activity
264 during the *Single Target* trials. **Figure 1a** shows the individual (middle panel) and mean log-
265 normalized EMG activity (right panel) during left-outward (orange trace), straight outward
266 (gray), and right-outward *Single Target* trials (green) from a representative participant. All trials
267 are aligned to visual target onset and the individual trials were sorted based on the reach RTs
268 (color squares). Note, the increase and decrease of activity in the right PEC muscle for left-
269 outward and right-outward reach movements, respectively. Consistent with previous studies
270 (Pruszynski et al., 2010; Wood et al., 2015), we observed a reliable difference in activity for the
271 three different reach directions at two epochs of neuromuscular activity: the initial SLR-epoch
272 that occurs ~100 ms after stimulus onset and the later MOV-epoch associated with reach RT
273 (stochastically occurring ~200 ms after stimulus onset). Across our participants, the mean ± SEM
274 discrimination time (see **Materials and Methods**) for the SLR was 87.7 ± 2.7 ms and the
275 corresponding reach RT was 232.2 ± 3.3 ms. We calculated the SLR magnitude for a given trial
276 as the mean log-normalized EMG activity during the SLR epoch as 85-125 ms after stimulus
277 onset (Gu et al., 2018, 2019, indicated by the white dashed boxes and shaded panels in **Fig. 1**).
278 For this participant, we found a reliable increase and decrease in SLR magnitude for left-outward
279 and right-outward trials, respectively, when compared to straight outward trials (1-way ANOVA,
280 $F_{(2,105)} = 37.41$, $P < 10^{-12}$, post-hoc Tukey's HSD, both $P < 0.001$).

281 Having established the profile of EMG activity during the SLR epoch on *Single Target*
282 trials, we next examined if the presence of a second non-chosen target on *Double Target* trials

283 changed the SLR. For a direct comparison with **Fig. 1a**, we first examined trials with the same
284 chosen (i.e. straight outward) target direction but with a different non-chosen target direction
285 (60° CW, blue, or 60° CCW, red, from the target, **Fig. 1b**). If the non-chosen target direction has
286 no influence (i.e. no averaging), we would predict that the SLR magnitude would resemble that
287 observed during outward reach movements during *Single Target* trials, which we overlaid in gray
288 in **Fig. 1b**. Despite the same chosen target direction, we observed an increase or decrease of
289 EMG activity during the SLR epoch for the *Double Target* trials relative to the *Single Target*
290 trials (1-way ANOVA, $F_{(2,83)} = 16.17$, $P < 10^{-5}$, post-hoc Tukey's HSD, $P = 0.01$ and $P = 0.004$,
291 respectively), if the non-chosen target lay in the left-outward or right-outward position,
292 respectively. This result suggests that EMG activity during the SLR is systematically altered by
293 the presence of the non-chosen target.

294 A second way to examine the SLR during *Double Target* trials is to compare SLR
295 magnitude on trials with the same two visual targets, but different chosen target directions.
296 **Figure 1c** shows the EMG activity when both the left-outward (blue) and right-outward (red)
297 targets were presented to the representative participant. If the SLR averaged the locations of the
298 two visual targets completely, then we would predict that the resulting EMG activity would
299 resemble that of an outward reach movement during *Single Target* trials (gray trace). However,
300 even though the same two visual targets appeared, we observed a reliable difference in SLR
301 magnitude depending on whether the participants chose either the left-outward or right-outward
302 target direction (1-way ANOVA, $F_{(2,72)} = 7.06$, $P = 0.002$, post-hoc Tukey's HSD, $P = 0.01$).
303 This result suggests that EMG activity during the SLR is modulated by the chosen target
304 direction, even when the same two visual targets are presented.

Systematic shifts in tuning of SLR during Double Target *trials*

The results from **Figure 1b** and **c** demonstrated that the magnitude of the SLR during *Double Target* trials depended on both the target configuration and the eventual chosen target direction. To quantify the extent of averaging that occurred, we sought to compare how the directional tuning of the SLR changed between *Single* and *Double Target* trials. Previously, it has been shown that the SLR magnitude can be well described by a cosine tuning function (Gu et al., 2019; **Eq. 1**). For each tuning function we can extract both the preferred direction (PD) and the amplitude of the fit. **Figure 2a** shows both the individual trial data (dots) and the cosine tuning fit (line) for the *Single Target* trials from the representative participant in **Fig. 1**. The PD of this fit was 173° CCW (arrow) from straight rightward, indicating that the largest SLR magnitude could be evoked by a visual stimulus presented straight leftward of the start position. Importantly, this cosine tuning between SLR magnitude and target direction was not simply due to movement-related EMG activity from trials with the shortest RTs: as this relationship was still presented when we performed a median RT split and re-fitted the data on either only *Fast RT* (**Fig. 2b**, dark line) or *Slow RT* trials (light), separately. Across our participants, we found no systematic differences in the PDs between *Fast* and *Slow RT* trials (**Fig. 2c**, group mean ± SEM: PD = 169° ± 3 and 162° ± 5°, respectively, paired *t*-test, $t_{(10)} = 1.30$, $P = 0.22$). We did find larger amplitude fits (i.e. larger SLR magnitude) for *Fast RT* compared to *Slow RT* trials (**Fig. 2d**, paired *t*-test, $t_{(10)} = 7.89$, $P < 10^{-4}$), which is consistent with previous studies demonstrating a negative correlation between SLR magnitudes and RTs on a trial-by-trial basis (Pruszynski et al., 2010; Gu et al., 2016). We will leverage this relationship later in the modeling portion of the **RESULTS**.

We next fitted the SLR magnitude for the *Double Target* trials. Note, we chose to align the trials based on the participant's chosen target direction (**Fig. 1b**) rather than controlling for the visual target locations (**Fig. 1c**) to accentuate the effect of the non-chosen target direction. **Figure 3a** shows the fits for the three different angular separations for the representative participant. For both the 60° and 120° conditions, we generated separate fits for when the non-chosen target direction was either CW (red) or CCW (blue) relative to the chosen target direction. The highlighted data (shaded box in the left panel of **Fig. 3a**) corresponds to the same trials as shown in **Fig. 1b**. The rightmost panel of **Fig. 3a** shows the fit of SLR magnitude to the 180° *Double Target* condition. Despite the two targets being in diametrically opposite directions, the SLR tuning during the 180° condition was still reliably tuned towards the chosen target direction similar to that observed in the *Single Target* trials (paired *t*-test, $t_{(10)} = 1.92$, $P = 0.08$). However, we did find a systematic decrease in the amplitude of the fits (see below).

For the 60° and 120° conditions, since we aligned our data relative to the chosen target direction, the only difference between CW and CCW trials was the non-chosen target direction. If the EMG activity was the result of a perfect averaging between the two target directions, then we would predict the difference in PD between CW and CCW trials (ΔPD) to be equal to the angular separation between the two targets (i.e. ΔPD = 60° and 120°, respectively). If the EMG activity was only influenced by the chosen target direction, then we would predict no difference between CW and CCW conditions (ΔPD = 0°). Consistent with the individual trial data from **Fig. 1b**, we observed signs of averaging, albeit incomplete, for the representative participant for both the 60° and 120° conditions, with ΔPDs = 49.3° and 53.0°, respectively (**Fig. 3a**).

We found similar results of partial averaging across our participants for both the 60° (**Fig. 3b**, left panel, mean ± SEM, ΔPD = 38.6° ± 3.5°, one sample *t*-test against zero, $t_{(10)} = 10.9$, $P <$

350 10^{-6}) and 120° *Double Target* conditions (ΔPD = 47.2 ± 5.4°, one sample *t*-test, $t_{(10)} = 8.7$, $P <$

351 10^{-5}). To directly compare the extent of averaging between the 60° and 120° conditions, we

352 converted the ΔPD into an averaging ratio (**Fig. 3b**, right panel): where a value of 1 indicates

353 complete averaging (ΔPD = 60° and 120°, dashed line in **Fig. 3b**) and a value of 0 indicates no

354 averaging (ΔPD = 0°). Overall, we found that the extent of averaging decreased as the angular

355 separation increased from 60° to 120° (averaging ratio = 0.64 ± 0.06 and 0.39 ± 0.05 a.u.,

356 respectively, paired *t*-test, $t_{(10)} = 3.81$, $P = 0.003$).

357 In addition to the changes in PD of the SLR magnitude, we also quantified the changes in

358 the amplitude of the fits during *Double Target* trials. **Figure 3c** shows the mean amplitude for

359 the three conditions normalized to each participant's own *Single Target* amplitude as a baseline.

360 We observed a systematic decrease in amplitude as a function of angular separation: 1.13 ± 0.04,

361 0.88 ± 0.04, and 0.63 ± 0.05 a.u. for the 60°, 120°, and 180° conditions, respectively (repeated

362 measures 1-way ANOVA, $F_{(2,20)} = 41.1$, $P < 10^{-7}$, post-hoc paired *t*-test, all $t_{(10)} > 5.5$, $P < 10^{-3}$).

363 These systematic changes in PD and amplitude will be interpreted based on different possible

364 averaging models tested below.

365

366 *Model predictions of EMG activity during the SLR epoch for* Double Target *trials*

367 Previous studies examining averaging behavior for both eye and reach movements have

368 proposed different models for how visual information from the two targets may be integrated

369 into a single motor command. These models make distinct predictions for how the PD and

370 amplitude of the cosine tuning should change between *Single* and *Double Target* trials (see

371 **MATERIALS AND METHODS** for exact details). **Figure 4e** shows the predicted cosine

372 tuning curves generated from the four different proposed models for both the 120° CW and

373 CCW conditions, using the *Single Target* data (dashed gray line) from the representative
374 participant shown in **Figs. 1** and **2**. **Model 1** is the *winner-takes-all model* (**Fig. 4a**), which
375 proposes that the two visual targets compete for selection in a winner-takes-all process, resulting
376 in a motor command that is generated towards the winning target direction (Donders, 1969;
377 McClelland, 1979). Effectively, there is no integration between the two targets direction at any
378 stage of the process. Note, this model is agnostic about whether the competition for selection
379 occurs at either a spatial or motor representation. **Model 2** is the *spatial averaging model* (**Fig.**
380 **4b**), which proposes that the two targets are first averaged into a single spatial representation,
381 resulting in a motor command towards the intermediate spatial direction (Findlay, 1982;
382 Glimcher and Sparks, 1993; Chou et al., 1999). **Model 3** is the *motor averaging model* (**Fig. 4c**),
383 which proposes that the two targets are first converted into their own motor command (Edelman
384 and Keller, 1996; Cisek and Kalaska, 2002; Port and Wurtz, 2003) and then averaged into a
385 single motor command (Katnani and Gandhi, 2011; Stewart et al., 2014; Gallivan et al., 2017).
386 Finally, **Model 4** is the *weighted motor averaging model* (**Fig. 4d**), which is a variation of the
387 motor averaging model. Once again, the two targets are first converted into two separate and
388 independent motor commands, but a stronger weighting is given towards the chosen compared to
389 the non-chosen target direction (Kim and Basso, 2008, 2010; Pastor-Bernier and Cisek, 2011).
390 The final motor command is an average of these two differentially weighted motor commands.
391 This model can be conceptualized as a race between two independent accumulators (Schall,
392 2001), with the eventual chosen motor command accumulating at a faster rate compared to the
393 non-chosen command. Instead of estimating the weights of the chosen and non-chosen target
394 direction, we used the *Fast RT* and *Slow RT* cosine tuning fits from the *Single Target* trials,
395 respectively. Previous studies (Gu et al., 2016, 2018) have linked SLR magnitude to the

396 ‘readiness’ of the motor system towards a specific target direction. Here, we assumed that during
397 *Double Target* trials the motor system chooses the more ‘ready’ target direction.

398 **Figure 5a** and **b** summarize the four different model predictions (color lines) for both the
399 changes in ΔPD averaging ratio and amplitude fits across the three different *Double Target*
400 angular separation conditions relative to *Single Target* trials. The *winner-takes-all model*
401 predicted no change in either ΔPD (i.e. averaging ratio = 0 a.u.) or amplitude (i.e. normalized
402 amplitude = 1 a.u.). Both the *spatial averaging* and *motor averaging models* predicted complete
403 averaging (i.e. averaging ratio = 1 a.u.). The key difference between the two models was the
404 predicted amplitude, where the *spatial averaging model* predicted no change (i.e. normalized
405 amplitude = 1 a.u.), while the *motor averaging model* predicted an overall decrease (i.e. < 1 a.u.).
406 Finally, the *weighted motor averaging model* predicted both a partial shift in PD (i.e. averaging
407 ratio between 0 and 1) and an overall decrease in amplitude. The extent of these changes
408 depended on each participant’s own *Fast RT* and *Slow RT* fits.

409 **Figure 5a** and **b** also shows our observed group data (white bars) plotted against the
410 predictions from the four models during the SLR epoch. Note, only the *weighted motor*
411 *averaging model* (green lines) captured both the systematic decrease in both the averaging ratio
412 and amplitude that was observed in the group data between the 60° and 120° *Double Target*
413 conditions. Since the parameters of all four models were derived from each participant’s own
414 *Single Target* trials and contained no free parameters, we can directly compare the four different
415 models. **Figure 5c** shows the mean ± SEM of the fit error between the observed and predicted
416 fits across the participants. We found that the *weighted motor averaging model* best predicted the
417 observed cosine tuning compared to the other three models during the SLR epoch (repeated
418 measures 1-way ANOVA, $F_{(3,30)} = 7.7$, $P < 10^{-3}$, post-hoc paired *t*-test, $t_{(10)} = 3.6$, 4.1, and 4.8, *P*

419 = 0.005, 0.002, and 0.0001, compared to the *winner-takes-all, spatial,* and *motor averaging*
420 *models*, respectively).
421
422 *Systematic repulsion away from the non-chosen target direction during MOV-related EMG*
423 *activity*
424 Up to this point, we have only examined the initial wave of EMG activity time-locked to the
425 onset of the two visual targets (i.e. during the SLR epoch). But how does the EMG activity
426 associated with movement onset (MOV) change during *Double Target* trials? Previous
427 behavioral studies have reported reach averaging by examining the initial reach direction to two
428 potential visual targets (Chapman et al., 2010; Stewart et al., 2014; Gallivan et al., 2017). Here,
429 we examined both EMG activity during the MOV epoch (i.e. mean EMG activity -20 to 20 ms
430 around reach onset), as well as the initial reach direction error.
431 **Figure 5d** and **e** show both the averaging ratio and amplitude fits for the participants
432 when we re-fitted cosine tuning fits for EMG activity during the MOV epoch. Unlike the SLR
433 epoch, the *winner-takes-all model* best predicted EMG activity around reach onset (**Fig. 5f**,
434 repeated measures 1-way ANOVA, $F_{(3,30)} = 348.8$, $P < 10^{-22}$, post-hoc paired *t*-test, $t_{(10)} = 28.6$,
435 21.8, 29.0, all $P < 10^{-9}$, compared to the *spatial, motor,* and *weighted motor averaging models*,
436 respectively). Although the winner-takes-all model provides the best best explanation for our
437 data, we still observe an influence of the non-chosen target in our data, but with an averaging
438 ratio shifting in the opposite direction, i.e. *away* from the non-chosen target direction (averaging
439 ratio = –0.13 ± 0.03 and –0.11 ± 0.01 a.u., for 60° and 120° *Double Target* trials, respectively,
440 one sample *t*-test against zero, $t_{(10)} = -4.2$ and –11.7, both $P < 0.05$, **Fig. 5d**). Thus, unlike

441 previous reaching experiments using the 'go-before-you-know' paradigm, we did not observe
442 reach averaging in the EMG activity during the MOV epoch.

443 This systematic repulsion away from the non-chosen target direction is also present in the
444 reach kinematics. **Figure 6a** shows the representative participant's initial reach error (i.e. the
445 difference between the chosen target direction and the initial reach direction at the time of reach
446 onset) for both *Single* and *Double Target* trials. We observed systematic shifts in median reach
447 error (vertical lines) away from the non-chosen target direction (red and blue circles along the *x*-
448 axis in **Fig. 6a**) for both the 60° and 120° *Double Target* conditions. **Figure 6b** shows the group
449 differences of the median initial reach error direction between the CW and CCW reach trials
450 (ΔInitial Reach Error = -25.7° ± 21.7° and -23.0° ± 2.6°, paired *t*-test, $t_{(10)}$ = -9.6 and -8.9, both P
451 $< 10^{-5}$, respectively). These reach error directions are consistent with the repulsion effect in ΔPD
452 observed during the MOV epoch (ΔPD = –7.5 ± 1.8 and –13.1 ± 1.1, for 60° and 120° *Double*
453 *Target* trials, respectively, **Fig. 6c**). Note, this repulsion effect is abolished at the end of the reach
454 movement (i.e. 10 cm away from the starting position, ΔFinal Reach Error = 0.05° ± 0.15° and
455 0.44° ± 0.19°, paired *t*-test, $t_{(10)}$ = 0.16 and 3.8, P = 0.88 and P = 0.004 in the opposite direction
456 as the initial reach error).
457

458 **DISCUSSION**

459 Contemporary theories of decision-making have suggested that the multiple potential motor
460 commands compete for action selection (Schall, 2001; Cisek, 2007). While there are clear
461 behavioral indications of such competition during saccadic averaging (He and Kowler, 1989;
462 Chou et al., 1999), where eye movements land in between two potential visual targets, there is an
463 ongoing debate on whether averaging occurs for reach movements (Chapman et al., 2010;

464 Gallivan et al., 2017; Wong and Haith, 2017). Here, by measuring the earliest wave of visually
465 evoked neuromuscular response (i.e. the *stimulus-locked response*) on an upper limb muscle
466 during a free-choice reach task, we observed averaging of two motor commands associated with
467 the two possible targets, similar to that observed previously for saccadic averaging. Further,
468 consistent with current theories of decision-making in motor control (Gallivan et al., 2018), we
469 observed a temporal transformation going from a competition between two different motor
470 commands during the SLR epoch (~100 ms after target onset) into a single goal-directed motor
471 command by the time of voluntary reach onset (~200-300 after target onset). Importantly, the
472 initial averaged motor command was biased towards the participant's chosen target direction on
473 a trial-by-trial basis.

474 We specifically chose to employ a free-choice reach task with an emphasis on short-
475 latency reach RTs. This task design, which has been proven successful in eliciting saccadic
476 averaging (see below for reach averaging paradigm), allowed a direct comparison between
477 saccadic averaging and a possible counterpart for reach movements. The averaged motor
478 response observed during the SLR epoch is reminiscent of the properties of saccadic averaging.
479 First, the greatest amount of saccadic averaging is seen for short-latency saccades (i.e. saccadic
480 RTs < 100 ms), while more goal-directed saccades occur for longer-latency RTs (Walker et al.,
481 1997; Chou et al., 1999). Similarly, we only observed reach averaging during the SLR but not
482 during the later MOV response. Second, in the saccadic system the extent of averaging decreases
483 as the angular separation increases between the two visual targets (Chou et al., 1999; Vokoun et
484 al., 2014). Again, we also observed larger reach averaging when the visual targets were 60°
485 rather than 120° apart.

486 The temporal separation between the SLR and the voluntary MOV epochs (Wood et al.,
487 2015) allowed us to examine how and at what potential stage of the sensorimotor transformation
488 the motor system may be averaging the two different potential targets. Classic saccadic
489 averaging studies have suggested that the brain first *spatially averages* the two visual stimuli and
490 then generates a motor command towards the intermediate direction (Coren and Hoenig, 1972;
491 Walker et al., 1997). In contrast, recent behavioral studies on reach averaging have suggested
492 that the brain averages the two different motor commands that are competing for selection
493 (Stewart et al., 2014; Gallivan et al., 2017), i.e. *motor averaging*. Due to the non-linear mapping
494 between the visual stimulus direction and the corresponding motor command, we could directly
495 test whether the averaging observed during the SLR epoch was the result of either spatial or
496 motor averaging (**Fig. 4**). Note, that we tested two different motor averaging models: (1) the
497 *motor averaging* model assumed that the two competing motor commands contributed equally to
498 the final averaged command, regardless of the final chosen target direction. In contrast, (2) the
499 *weighted motor averaging* model assumed that the initial competition between the two targets
500 was biased (Kim and Basso, 2010; Pastor-Bernier and Cisek, 2011) towards the eventual chosen
501 target, thus resulting in a larger weighting for the motor response corresponding to the chosen
502 compared to the non-chosen target. To estimate the weighting of the chosen and non-chosen
503 targets for each participant, we used the difference in SLR magnitude between fast and slow RT
504 trials during the *Single Target* trials (see **MATERIALS AND METHODS**).
505 We found that the *weighted motor averaging model* explained the SLR magnitude better
506 than any of the other models (**Fig. 5**). This result is consistent with contemporary theories of
507 decision-making for multiple competing motor plans (Schall, 2001; Cisek, 2007). For example,
508 previous neurophysiological studies have shown that experimentally manipulating the decision

variable through either target uncertainty (Basso and Wurtz, 1997; Dorris and Munoz, 1998), target expectation (Bichot et al., 1996; Basso and Wurtz, 1998), or reward expectation (Rezvani and Corneil, 2008; Pastor-Bernier and Cisek, 2011) modulates the neural presentation of the competing motor commands. Here, rather than experimentally manipulating biases we exploited the fact that participants randomly choose one of the two visual targets and demonstrated post-hoc that the averaged SLR magnitude was biased towards the eventual chosen target direction *Double Target* trials. This suggests that random fluctuations along the sensorimotor pathway (Faisal et al., 2008) or idiosyncratic preferences based on earlier choices bias the competition process and thus influence the final decision.

Our results pertain to recent findings debating whether neural activity in dorsal premotor cortex represents two potential targets simultaneously (Cisek and Kalaska, 2005; Klaes et al., 2011) or whether such results arise from combining single-trial data representing either one of two locations across multiple trials (Dekleva et al., 2018). Our results clearly show an influence of a competition between both targets on the earliest wave of EMG activity on a trial-by-trial basis. Note that our results are based on the initial visual transient response, which previous neurophysiological studies have specifically excluded and only examined the delay activity for any potential motor actions.

While our SLR results are consistent with earlier kinematic results of reach averaging studies (Stewart et al., 2014; Gallivan et al., 2017), these studies have suggested that motor averaging should also leak out to the reach kinematics at the time of reach onset. However, in our study there was no indication of motor averaging in the reach kinematics. Instead, the error in the initial reach direction was systematically *away* from the non-chosen target direction, which was also supported by the observed shift in the PD of EMG activity at the time of reach onset

532 (**Fig. 6**). This repulsion effect disappeared when we examined the final reach error, thus
533 suggesting that participants were actively generating curved reach movements away from the
534 non-chosen target direction. While counterintuitive, this observation is in line with previous
535 reach studies (Chapman and Goodale, 2008, 2010; de Haan et al., 2014) that reported curved
536 movements away from a visual stimulus that was defined as an obstacle rather than a target. Our
537 current results suggest that by the onset of reach initiation (~200-300 ms after stimuli onset)
538 participants have already decided which target to reach towards and they have also incorporated
539 a strategy to actively avoid the non-chosen target direction (Wong and Haith, 2017).
540 In summary, we examined neuromuscular activity during a reach version of free-choice
541 task that has previously been shown to elicit saccadic averaging. We found that similar to
542 saccadic averaging, the initial short-latency reach motor command (i.e. the SLR) is a behavioral
543 indicator of an incomplete competition of two distinct motor plans. However, this competition is
544 rapidly resolved and the motor system then generates a strategic motor plan that is optimal for
545 the current task demands.
546

547 **AUTHOR CONTRIBUTIONS**

548 Conceptualization – CG, BDC, LPS, and WPM; Methodology – CG and LPS; Investigation –
549 CG; Writing, Original Draft – CG and LPS; Writing, Review and Editing – BDC, LPS, and
550 WPM; Funding Acquisition – CG and WPM; Resources – WPM; Supervision – BDC, LPS, and
551 WPM.

552 **DECLARATION OF INTERESTS**

553 The authors declare no competing interesting.

554 **References**

555 Basso MA, Wurtz RH (1997) Modulation of neuronal activity by target uncertainty. Nature
556 389:66–69.

557 Basso MA, Wurtz RH (1998) Modulation of neuronal activity in superior colliculus by changes
558 in target probability. Journal of Neuroscience 18:7519–7534.

559 Bichot NP, Schall JD, Thompson KG (1996) Visual feature selectivity in frontal eye fields
560 induced by experience in mature macaques. Nature 381:697–699.

561 Bichot NP, Thompson KG, Rao SC, Schall JD (2001) Reliability of Macaque Frontal Eye Field
562 Neurons Signaling Saccade Targets during Visual Search. J Neurosci 21:713–725.

563 Chapman BB, Corneil BD (2011) Neuromuscular recruitment related to stimulus presentation
564 and task instruction during the anti-saccade task. The European Journal of Neuroscience
565 33:349–360.

566 Chapman CS, Gallivan JP, Wood DK, Milne JL, Culham JC, Goodale MA (2010) Reaching for
567 the unknown: multiple target encoding and real-time decision-making in a rapid reach
568 task. Cognition 116:168–176.

569 Chapman CS, Goodale MA (2008) Missing in action: the effect of obstacle position and size on
570 avoidance while reaching. Exp Brain Res 191:83–97.

571 Chapman CS, Goodale MA (2010) Obstacle avoidance during online corrections. Journal of
572 Vision 10:17.

573 Chou IH, Sommer MA, Schiller PH (1999) Express averaging saccades in monkeys. Vision
574 Research 39:4200–4216.

575 Cisek P (2007) Cortical mechanisms of action selection: the affordance competition hypothesis.
576 Philosophical transactions of the Royal Society of London Series B, Biological sciences
577 362:1585–1599.

578 Cisek P, Kalaska JF (2002) Simultaneous Encoding of Multiple Potential Reach Directions in
579 Dorsal Premotor Cortex. Journal of Neurophysiology 87:1149–1154.

580 Cisek P, Kalaska JF (2005) Neural Correlates of Reaching Decisions in Dorsal Premotor Cortex:
581 Specification of Multiple Direction Choices and Final Selection of Action. Neuron
582 45:801–814.

583 Coren S, Hoenig P (1972) Effect of Non-Target Stimuli upon Length of Voluntary Saccades.
584 Perceptual and Motor Skills 34:499–508.

585 Corneil BD, Olivier E, Munoz DP (2004) Visual responses on neck muscles reveal selective
586 gating that prevents express saccades. Neuron 42:831–841.

587 Cui H, Andersen RA (2011) Different representations of potential and selected motor plans by
588 distinct parietal areas. Journal of Neuroscience 31:18130–18136.

589 de Haan AM, Van der Stigchel S, Nijnens CM, Dijkerman HC (2014) The influence of object
590 identity on obstacle avoidance reaching behaviour. Acta Psychologica 150:94–99.

591 Dekleva BM, Kording KP, Miller LE (2018) Single reach plans in dorsal premotor cortex during
592 a two-target task. Nature Communications 9:3556.

593 Donders FC (1969) On the speed of mental processes. Acta psychologica 30:412–31.

594 Dorris MC, Munoz DP (1998) Saccadic Probability Influences Motor Preparation Signals and
595 Time to Saccadic Initiation. The Journal of neuroscience : the official journal of the
596 Society for Neuroscience 18:7015–26.

597 Edelman JA, Keller EL (1996) Activity of visuomotor burst neurons in the superior colliculus
598 accompanying express saccades. Journal of Neurophysiology 76:908–926.

599 Faisal AA, Selen LPJ, Wolpert DM (2008) Noise in the nervous system. Nature Reviews
600 Neuroscience 9:292–303.

601 Findlay JM (1982) Global visual processing for saccadic eye movements. Vision Research
602 22:1033–1045.

603 Gallivan JP, Chapman CS, Wolpert DM, Flanagan JR (2018) Decision-making in sensorimotor
604 control. Nat Rev Neurosci 19:519–534.

605 Gallivan JP, Stewart BM, Baugh LA, Wolpert DM, Flanagan JR (2017) Rapid Automatic Motor
606 Encoding of Competing Reach Options. Cell Reports 18:1619–1626.

607 Glimcher PW, Sparks DL (1993) Representation of averaging saccades in the superior colliculus
608 of the monkey. Experimental Brain Research 95:429–435.

609 Gu C, Pruszynski JA, Gribble PL, Corneil BD (2018) Done in 100 ms: path-dependent
610 visuomotor transformation in the human upper limb. Journal of Neurophysiology
611 119:1319–1328.

612 Gu C, Pruszynski JA, Gribble PL, Corneil BD (2019) A rapid visuomotor response on the human
613 upper limb is selectively influenced by implicit motor learning. Journal of
614 Neurophysiology 121:85–95.

615 Gu C, Wood DK, Gribble PL, Corneil BD (2016) A Trial-by-Trial Window into Sensorimotor
616 Transformations in the Human Motor Periphery. Journal of Neuroscience 36:8273–8282.

617 He P, Kowler E (1989) The role of location probability in the programming of saccades:
618 Implications for “center-of-gravity” tendencies. Vision Research 29:1165–1181.

619 Howard IS, Ingram JN, Wolpert DM (2009) A modular planar robotic manipulandum with end-
620 point torque control. Journal of Neuroscience Methods 181:199–211.

621 Hudson TE, Maloney LT, Landy MS (2007) Movement Planning With Probabilistic Target
622 Information. Journal of Neurophysiology 98:3034–3046.

623 Katnani HA, Gandhi NJ (2011) Order of operations for decoding superior colliculus activity for
624 saccade generation. Journal of Neurophysiology 106:1250–1259.

625 Kim B, Basso MA (2008) Saccade target selection in the superior colliculus: a signal detection
626 theory approach. Journal of Neuroscience 28:2991–3007.

627 Kim B, Basso MA (2010) A Probabilistic Strategy for Understanding Action Selection. Journal
628 of Neuroscience 30:2340–2355.

629 Klaes C, Westendorff S, Chakrabarti S, Gail A (2011) Choosing Goals, Not Rules: Deciding
630 among Rule-Based Action Plans. Neuron 70:536–548.

631 McClelland JL (1979) On the time relations of mental processes: An examination of systems of
632 processes in cascade. Psychological Review 86:287–330.

633 McPeek RM, Keller EL (2002) Saccade target selection in the superior colliculus during a visual
634 search task. Journal of Neurophysiology 88:2019–2034.

635 Ottes FP, Van Gisbergen JAM, Eggermont JJ (1984) Metrics of saccade responses to visual
636 double stimuli: Two different modes. Vision Research 24:1169–1179.

637 Pastor-Bernier A, Cisek P (2011) Neural Correlates of Biased Competition in Premotor Cortex.
638 Journal of Neuroscience 31:7083–7088.

639 Port NL, Wurtz RH (2003) Sequential Activity of Simultaneously Recorded Neurons in the
640 Superior Colliculus During Curved Saccades. Journal of neurophysiology 90:1887–1903.

641 Pruszynski JA, King GL, Boisse L, Scott SH, Flanagan JR, Munoz DP (2010) Stimulus-locked
642 responses on human arm muscles reveal a rapid neural pathway linking visual input to
643 arm motor output. The European Journal of Neuroscience 32:1049–1057.

644 Rezvani S, Corneil BD (2008) Recruitment of a head-turning synergy by low-frequency activity
645 in the primate superior colliculus. Journal of Neurophysiology 100:397–411.

646 Schall JD (2001) Neural basis of deciding, choosing and acting. Nature Reviews Neuroscience
647 2:33–42.

648 Stewart BM, Gallivan JP, Baugh LA, Flanagan JR (2014) Motor, not visual, encoding of
649 potential reach targets. Current Biology 24:R953–4.

650 Vokoun CR, Huang X, Jackson MB, Basso MA (2014) Response Normalization in the
651 Superficial Layers of the Superior Colliculus as a Possible Mechanism for Saccadic
652 Averaging. Journal of Neuroscience 34:7976–7987.

653 Walker R, Deubel H, Schneider WX, Findlay JM (1997) Effect of remote distractors on saccade
654 programming: evidence for an extended fixation zone. Journal of neurophysiology
655 78:1108–1119.

656 Wong AL, Haith AM (2017) Motor planning flexibly optimizes performance under uncertainty
657 about task goals. Nature Communications 8:14624.

658 Wood DK, Gu C, Corneil BD, Gribble PL, Goodale MA (2015) Transient visual responses reset
659 the phase of low-frequency oscillations in the skeletomotor periphery. The European
660 Journal of Neuroscience 42:1919–1932.

661

FIGURE LEGENDS

Figure 1: SLR from a representative participant. a. Individual (middle panel) and mean ± SEM (right) log-normalized EMG activity from the right PEC muscle during left-outward (yellow), straight outward (gray), and right-outward (green) *Single Target* reach trials. All EMG activity is aligned to the onset of the peripheral visual target (thick black vertical line). For individual trials, each row represents EMG activity with a single trial and trials were sorted based on reach RT (color squares). Dashed white box and shaded panel in the individual and mean EMG plots represent the SLR epoch (85-125 ms after stimulus onset). **b.** EMG activity for *Double Target* trials when matched for the same outward reach movement. The non-chosen target was either 60° CW (blue) or CCW (red) of the reach target. Same layout as **a**. **c.** EMG activity for 120° *Double Target* trials with the same left-outward and right-outward visual targets. The trials were sorted based on the chosen target direction. Same layout as **a**. * $P < 0.05$.

Figure 2: Directional tuning of the SLR during *Single Target* trials. a. Cosine tuning of log-normalized SLR magnitude as a function of the target reach direction for *Single Target* trials from the representative participant in **Fig. 1**. Dots indicate each trial, the solid line indicates the fit, and the arrow indicates the PD of the fit. **b.** The cosine tuning is maintained regardless of the ensuing reach RT, same data as **a**. but re-fitted for *Fast* (black) and *Slow RT* (gray) *Single Target* trials separately. For illustration purposes only, we have staggered the individual trial data to illustrate the difference between the two conditions. We did not stagger the cosine tuning curves. **c, d.** Group (n = 11) mean ± SEM for the PD (**c**) and amplitude (**d**) of the fits between the *Fast* and *Slow RT* trials. Each gray line indicates an individual participant and the darker line indicates the representative participant. * $P < 0.05$.

Figure 3: Systematic changes in directional tuning of the SLR during *Double Target* trials. a. Fits for 60°, 120°, and 180° conditions of the *Double Target* trials with all data aligned to the chosen target direction from the representative participant. For both the 60° and 120° conditions, the trials were sorted based on whether the non-chosen target was either CW (blue) or CCW (red) of the chosen target direction., Data in the shaded panel indicates the same trials from **Fig. 1b**. **b.** Group mean ± SEM shifts in PD (ΔPD) between the CW and CCW trials (left panel) and the normalized averaging ratio (right) for both 60° and 120° conditions across our participants. Dashed box indicates the predicted ΔPD the SLR completely averaged the two targets (averaging ratio = 1 a.u.). **c.** Mean ± SEM amplitude of the fits for the three different *Double Target* conditions across our participants. The amplitudes were normalized to each participant's own amplitude fit from the *Single Target* trials. Each grey line indicates a different participant and the darker line indicates the representative participant from **a**. * $P < 0.05$.

Figure 4: Model predictions of the tuning curves during *Double Target* trials. a. The *winner-takes-all* model chooses one visual stimulus as the target and converts it into the final motor command. **b.** The *spatial averaging* model averages the two visual stimulus directions into an intermediate target direction and that target direction is converted into a motor command. **c.** The *motor averaging* model first converts the two visual stimuli into two separated motor commands. Then it averages the two motor commands into a single motor command. **d.** The *weighted motor averaging* model first converts the two visual stimuli into two separate motor commands, but the cosine tuning have different weights. Then it averages the two motor commands into a single

motor command. **e.** The predicted tuning curves for 120° *Double Target* trials from the representative participants in **Figs. 1** and **2**.

Figure 5: Comparisons of model predictions and observed group data for *Double Target* trial fits. a, b. The model predictions (color lines) overlaid over the observed mean ± SEM group data (open black bars) for EMG activity during the SLR epoch (85-125 ms after stimuli onset) for both the averaging ratio (**a**) and amplitude (**b**). **c.** The mean ± SEM group model fit errors for the four different models. **d-f.** Same analysis as **a-c.** but examining the EMG activity during the MOV epoch (-20-20 ms around reach RT). * $P < 0.0083$.

Figure 6: Systematic repulsion away from the non-chosen target direction at the time of reach RT. a. Histogram of reach error direction, relative to the chosen target direction) at the time of reach RT for the representative participant during the experiment. For *Double Target* trials, the location of the non-chosen target direction is shown as colored circles along the *x*-axis. Vertical lines represent the median reach errors. **b.** Mean ± SEM of difference in median reach error between CW and CCW during *Double Target* trials. **c.** Mean ± SEM of ΔPD during the MOV epoch. Same layout as left panel in **Fig. 3b**.

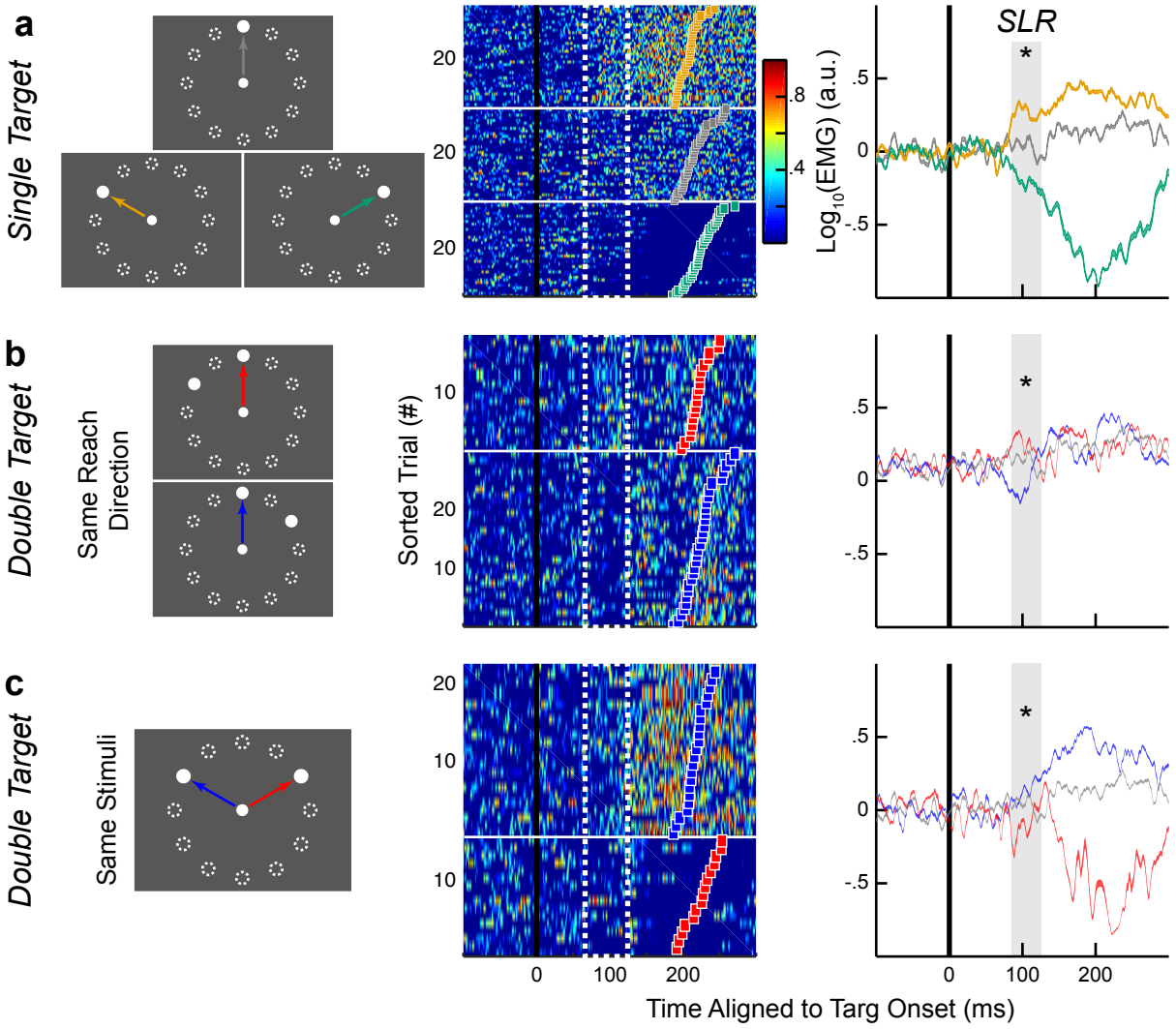
a
Single Target
b
Double Target
Same Reach Direction
c
Double Target
Same Stimuli
Sorted Trial (#)
20
20
20
10
20
10
20
10
10
.8
.4
SLR
*
Log10(EMG) (a.u.)
.5
0
-.5
0
100
200
Time Aligned to Targ Onset (ms)

Figure 1

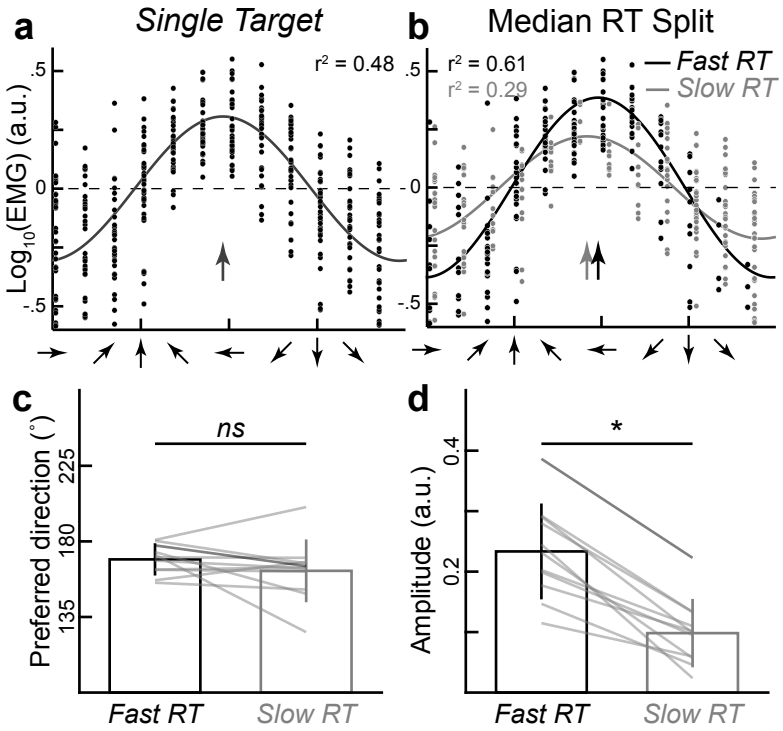
a
Single Target
b
Median RT Split
r² = 0.48
r² = 0.61
r² = 0.29
Fast RT
Slow RT
Log10(EMG) (a.u.)
.5
0
-.5
c
d
ns
*
Preferred direction (°)
225
180
135
Amplitude (a.u.)
0.4
0.2
Fast RT
Slow RT

Figure 2

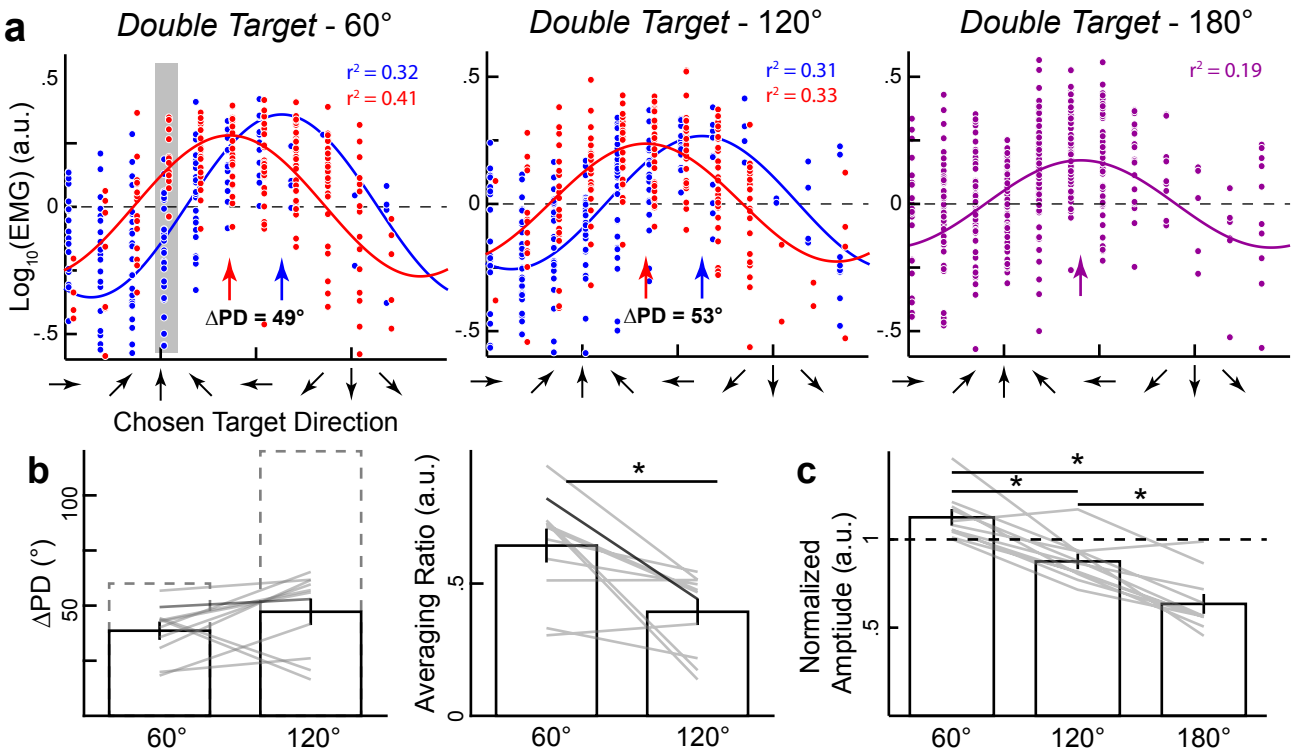
a
Double Target - 60°
Double Target - 120°
Double Target - 180°
r² = 0.32
r² = 0.41
r² = 0.31
r² = 0.33
r² = 0.19
ΔPD = 49°
ΔPD = 53°
Log10(EMG) (a.u.)
.5
0
-.5
Chosen Target Direction
b
ΔPD (°)
100
50
60°
120°
Averaging Ratio (a.u.)
.5
0
*
c
Normalized Amptiude (a.u.)
1
.5
*
*
*
60°
120°
180°

Figure 3

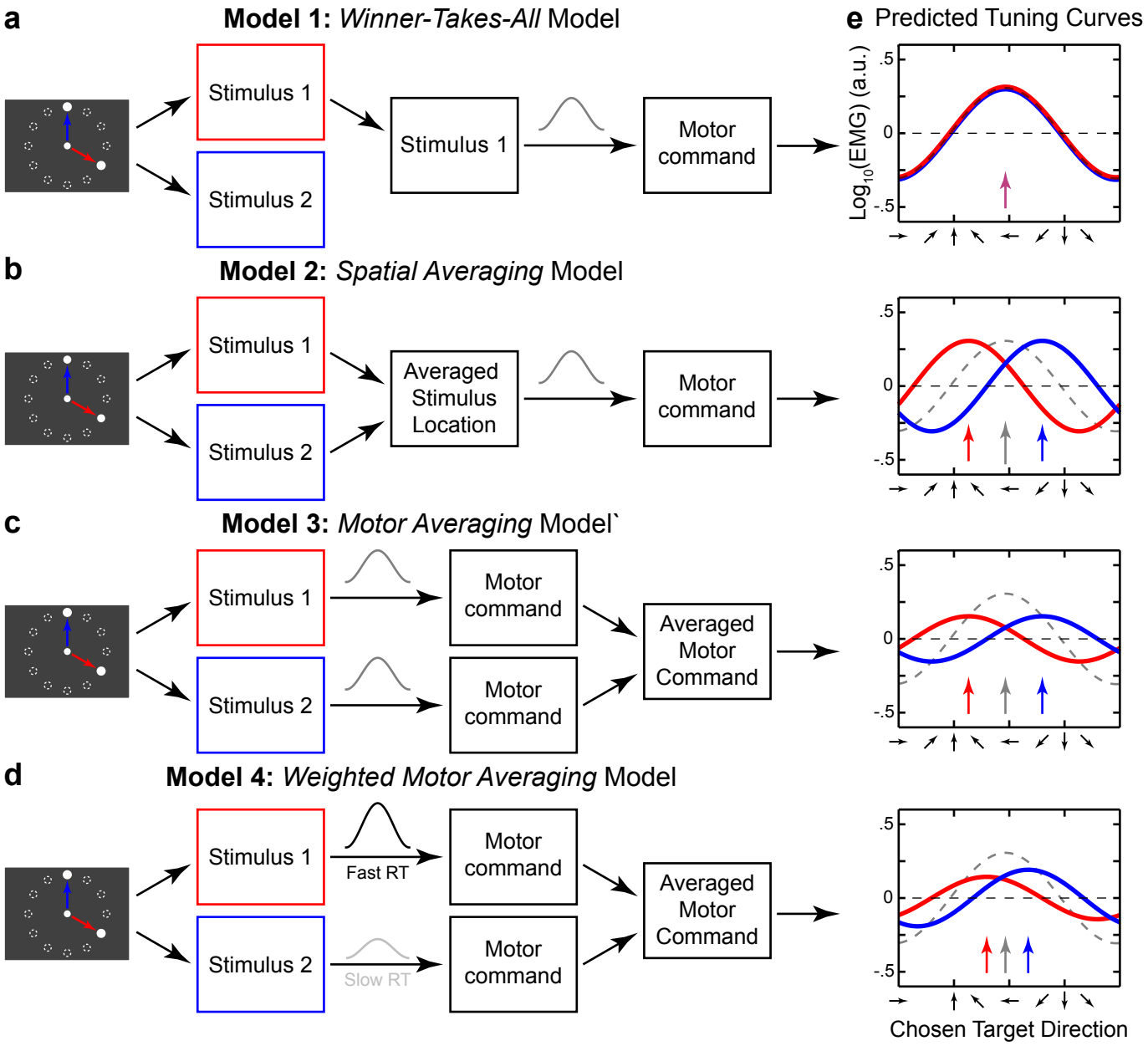
a
Model 1: Winner-Takes-All Model
e Predicted Tuning Curves
Stimulus 1
Stimulus 2
Stimulus 1
Motor command
Log10(EMG) (a.u.)
.5
0
-.5
b
Model 2: Spatial Averaging Model
Stimulus 1
Stimulus 2
Averaged Stimulus Location
Motor command
c
Model 3: Motor Averaging Model`
Stimulus 1
Stimulus 2
Motor command
Motor command
Averaged Motor Command
d
Model 4: Weighted Motor Averaging Model
Stimulus 1
Stimulus 2
Fast RT
Slow RT
Motor command
Motor command
Averaged Motor Command
Chosen Target Direction

Figure 4

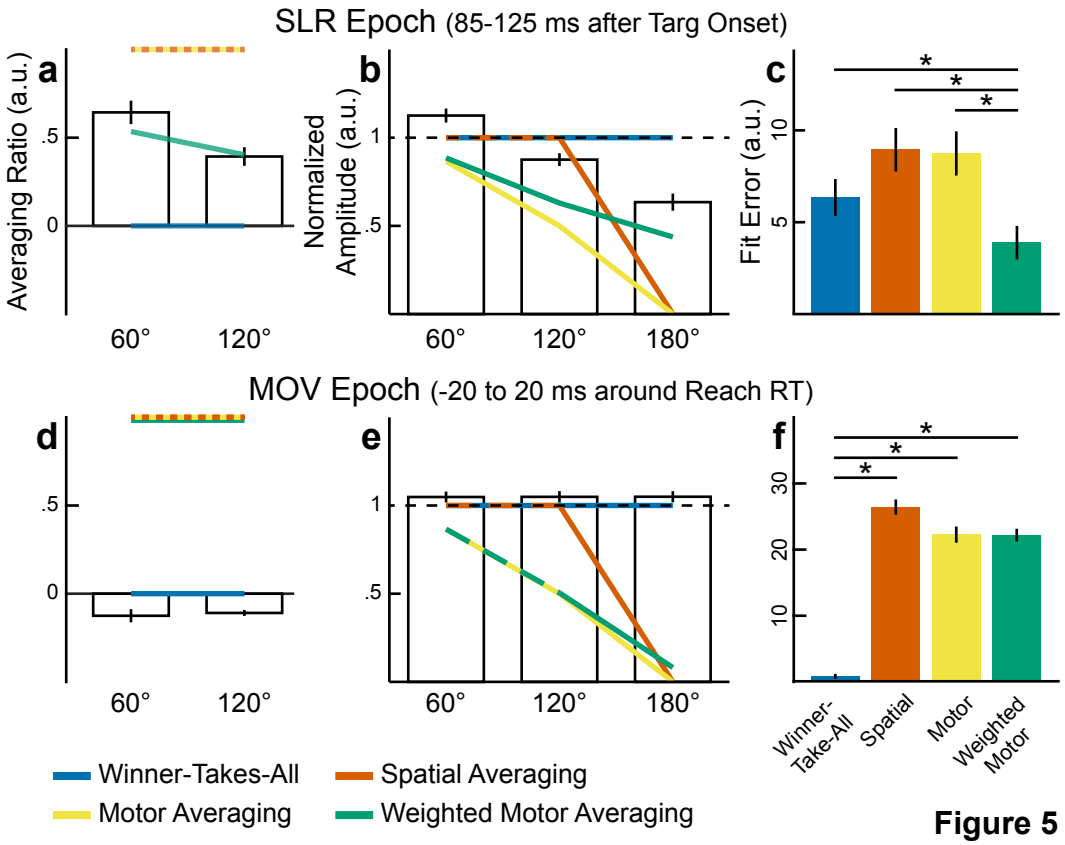
SLR Epoch (85-125 ms after Targ Onset)
a
Averaging Ratio (a.u.)
.5
0
60°
120°
b
Normalized Amplitude (a.u.)
1
.5
60°
120°
180°
c
Fit Error (a.u.)
10
5
*
*
*
MOV Epoch (-20 to 20 ms around Reach RT)
d
.5
0
60°
120°
e
1
.5
60°
120°
180°
f
30
20
10
*
*
*
Winner-Take-All
Spatial
Motor
Weighted Motor
Winner-Takes-All
Spatial Averaging
Motor Averaging
Weighted Motor Averaging

Figure 5

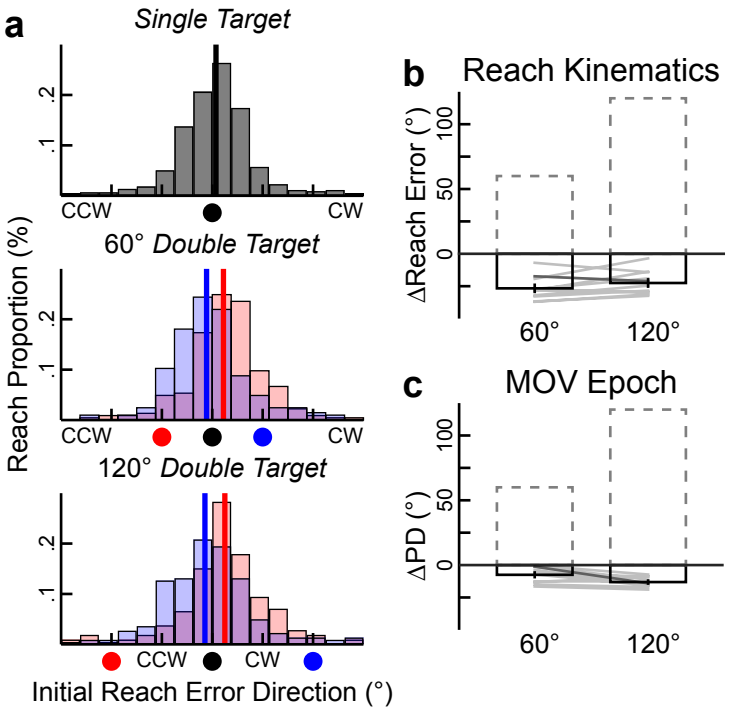
a
Single Target
.2
.1
CCW
CW
60° Double Target
Reach Proportion (%)
120° Double Target
Initial Reach Error Direction (°)
b
Reach Kinematics
ΔReach Error (°)
100
50
0
60°
120°
c
MOV Epoch
ΔPD (°)

Figure 6